Journal of Biomolecular NMR, **26:** 249–257, 2003.
KLUWER/ESCOM

Observation of a distinct transition in the mode of interconversion of ring pucker conformers in non-crystalline D-ribose-2′-*d* from ^{2}H NMR spin-alignment

Andy C. LiWang[a,*], David E. McCready[b], Gary P. Drobny[c], Brian R. Reid[c] & Michael A. Kennedy[d,*]

[a]*Department of Biochemistry & Biophysics, Texas A&M University, 2128 TAMU, College Station, TX 77843-2128, U.S.A.;* [b]*Interfacial and Nano Science Facility, and* [d]*Macromolecular Structure & Dynamics, Biological Sciences Laboratory, Pacific Northwest National Laboratory, EMSL 2569, K8-98, Richland, WA 99352, U.S.A.;* [c]*Department of Chemistry, University of Washington, Seattle, WA 98195-1700, U.S.A.*

Received 12 February 2003; Accepted 21 March 2003

Key words: Arrhenius, deuterium, internal motions, ribose, solid state NMR, spin alignment, X-ray diffraction

Abstract

Internal motions of D-ribose selectively ^{2}H-labeled at the 2′ position were measured using solid state ^{2}H NMR experiments. A sample of D-ribose-*2′-d* was prepared in a hydrated, non-crystalline state to eliminate effects of crystal-packing. Between temperatures of −74 and −60 °C the C2′–H2′ bond was observed to undergo two kinds of motions which were similar to those of C2′–H2′/H2″ found previously in crystalline deoxythymidine (Hiyama et al. (1989) *J. Am. Chem. Soc.*, **111**, 8609–8613): (1) Nanosecond motion of small angular displacement with an apparent activation energy of 3.6 ± 0.7 kcal mol^{-1}, and (2) millisecond to microsecond motion of large amplitude with an apparent activation energy ≥4 kcal mol^{-1}. At −74 °C, the slow, large-amplitude motion was best characterized as a two-site jump with a correlation time on the millisecond time scale, whereas at −60 °C it was diffusive on the microsecond time scale. The slow, large-amplitude motions of the C2′–H2′ bond are most likely from interconversions between C2′-*endo* and C3′-*endo* by way of the O4′-*endo* conformation, whereas the fast, small-amplitude motions are probably librations of the C2′–H2′ bond within the C2′-*endo* and C3′-*endo* potential energy minima.

Introduction

Furanose ring puckering and conformational flexibility is fundamental to the structure and function of nucleic acids (Saenger, 1984). The conformations and dynamics of furanose in RNA and DNA have been investigated for many years. X-ray crystallographic studies have shown that the sugar rings of RNA and DNA tend to cluster at the C3′-*endo* and C2′-*endo* conformations (Saenger et al., 1986; Dickerson, 1983; Arnott and Hukins, 1972) but there is substantial experimental evidence that the furanose ring is dynamic (Kojima et al., 1998; Bax and Lerner, 1988) in a sequence-dependent manner (Robinson et al., 1997; Hatcher et al., 1998; Meints et al., 2001). Whether the interconversion proceeds via a diffusive or jump process is related to intervening energy barriers, which, in turn, are dependent on the nature of the substituents and remain debated (Roder et al., 1975; Levitt and Warshel, 1978; Olson, 1982; Olson and Sussman, 1982).

From studies of small model compounds, estimates of the energy barrier of interconversion between the C2′-*endo* and C3′-*endo* conformations range from 0.5–5 kcal mol^{-1}. Deoxyribose ring flexibility was examined in crystalline deoxythymidine-2′-*C*,2″-*C*-d_2 using solid state ^{2}H NMR (Hiyama et al., 1989) and was found to execute two kinds of internal mo-

*To whom correspondence should be addressed. E-mails: andy-liwang@tamu.edu; ma_kennedy@pnl.gov

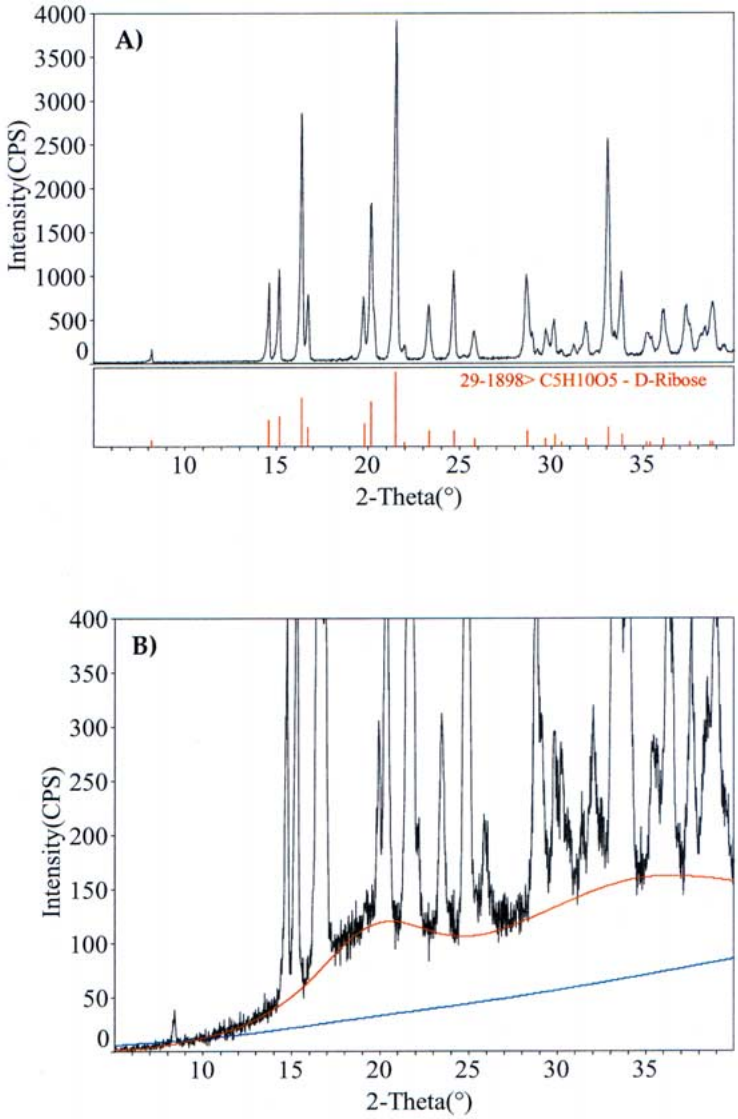

Figure 1. X-ray powder diffraction data of D-ribose at −20 °C. A) Anhydrous D-ribose is shown on top and below in red is reference data (Powder Diffraction File PDF-2 Database (2002) PDF 29-1898, JCPDS-ICDD). B) Hydrated D-ribose. The fitted background (red) indicates the amorphous component whereas the blue line indicates the fully crystalline, anhydrous component.

tion: (1) Small amplitude (≤5° r.m.s.) librations on the nanosecond time scale and (2) large amplitude jumping motions (≥30° r.m.s.) on the millisecond to microsecond time scale. The former motion was hypothesized to be exchange between the C3′-*exo* and C2′-*endo* conformations, whereas the latter motion was postulated to be C2′-*endo* ↔ C3′-*endo* interconversions. However, the large-amplitude motion was sensitive to crystal-packing forces (Hiyama et al., 1989). Furthermore, several solid-state ^{2}H NMR studies have shown that furanose ring dynamics in DNA is sequence dependent and can be either diffusive or occur by jump motions (Hatcher et al., 1998; Meints et al., 2001). Existing liquid and solid-state NMR data related to sugar ring puckering and energetics come from ribose and deoxyribose with a variety of substituents, from within DNA and RNA in a variety of sequence contexts, and, in some solid-state studies, have been influenced by crystal packing forces. To date there has been no experimental NMR characterization of dynamics of simple unsubstituted ribose in the solid-state. Here, we characterize the internal mo-

tions of hydrated non-crystalline D-ribose deuterated at the 2′ position (D-ribose-*2′-d*) using solid state ^{2}H NMR experiments in an effort to elucidate fundamental dynamic and energetic properties of this important biological building block.

Methods

X-ray diffraction

X-ray powder diffraction data were recorded for both anhydrous and partially hydrated D-ribose. The hydrated sample material used for X-ray analysis was prepared by placing anhydrous D-ribose in a closed chamber containing an excess of solid $NaNO_2$ in contact with a saturated solution of $NaNO_2$ (66% relative humidity, Weast (1988)) for two days. Weight measurements of the ribose sample before and after hydration indicated that there was an average of 1.4 waters per ribose molecule. The hydrated sample was in the form of a wet paste, so no further sample preparation was performed except to mount it in the sample holder. Samples of D-ribose when left in the humidity chamber for approximately one week were observed to completely deliquesce.

The X-ray diffraction apparatus used in this study was a Philips X'Pert MPD system (PW3040/00 type). The X-ray source was a sealed ceramic tube operated at 45 kV, 40 mA (λ = Cu $K_{\alpha 1}$, 1.5406 Å). The study specimens were examined in Bragg-Brentano parafocusing geometry on a 220-mm θ-θ goniometer radius using incident- and diffracted-beam soller slits (0.04 radians), automatic divergence and anti-scatter slits (10-mm irradiation length), and a 0.2-mm receiving slit. Wavelength selection was achieved with a curved graphite diffracted beam monochromator, and the detection apparatus was a Xe-filled sealed proportional counter.

A liquid nitrogen-cooled Anton-Paar TTK 450 low-temperature chamber was attached to the diffractometer to facilitate measurements under subambient conditions. This sample chamber utilizes front-loading specimen holders constructed of Ni-plated copper. The X-ray beam spot (approximately 10 mm $\times$ 10 mm throughout the scan range) was confined to the surface of the study material. The Anton-Paar TTK 450 chamber was purged with ultrahigh purity helium during this study to prevent condensation and icing.

Both the diffractometer and sample chamber were controlled using the Philips X'Pert software suite (X'Pert Data Collector, V1.3d). The scan range was 5.00°–40.00° 2θ collected at a rate of 0.02° s^{-1}. Analysis of the experimental patterns was accomplished using Jade V6.5.7 (Materials Data, Inc., Livermore, CA) and the Powder Diffraction File database (PDF-2, 2002 Release, International Centre for Diffraction Data, Newtown Square, PA).

NMR spectroscopy

Two-hundred milligrams of D-ribose-*2′-d* were packed into a 5 mm $\times$ 15 mm glass tube and placed in a chamber with an atmosphere at 66% relative humidity using ^{2}H-depleted ^1H_2O (Wang et al., 1992; Weast, 1988) until there was an average of 3.1 waters per ribose molecule, as determined from weight measurements. The sample was also in the form of a wet paste. All experiments were performed at 61.4 MHz ^{2}H Larmor frequency using a homebuilt spectrometer (Gladden and Drobny, unpublished results).

^{2}H NMR spectra of D-ribose-*2′-d* were recorded using an eight-step phase-cycled quadrupole echo pulse sequence (Davis et al., 1976). The 90° pulses were typically 2–3 μs in length and τ_1 = 25 μs. Data acquisition was initiated prior to the top of the quadrupole echo. The time domain data were left-shifted to the echo maximum, and Lorentzian line broadening of 2–3 kHz was applied to the free induction decay prior to Fourier transformation. Spin alignment echo experiments (Lausch and Spiess, 1980; Spiess, 1980) were carried out using a period of τ_1 = 25 μs between the first and second pulses while the delay between the second and third pulses, τ_2, was varied from 0 to 300 ms.

Powder averaged spin-lattice ^{2}H relaxation times of D-ribose-*2′-d*, $\langle T_1 \rangle$, were measured as a function of temperature using a saturation-recovery pulse sequence consisting of a comb of 90^o pulses separated by short delays ($\ll \langle T_1 \rangle$) and followed, after a variable recovery period, by a quadrupole echo sequence. The recovered magnetization was measured from the height of the quadrupole echo. The heights were plotted against the recovery period and $\langle T_1 \rangle$ values were determined using non-linear least squares fits to the data assuming single exponential recovery.

Results and discussion

Anhydrous D-ribose-*2′-d* exhibited extremely long deuterium spin-lattice relaxation times (data not

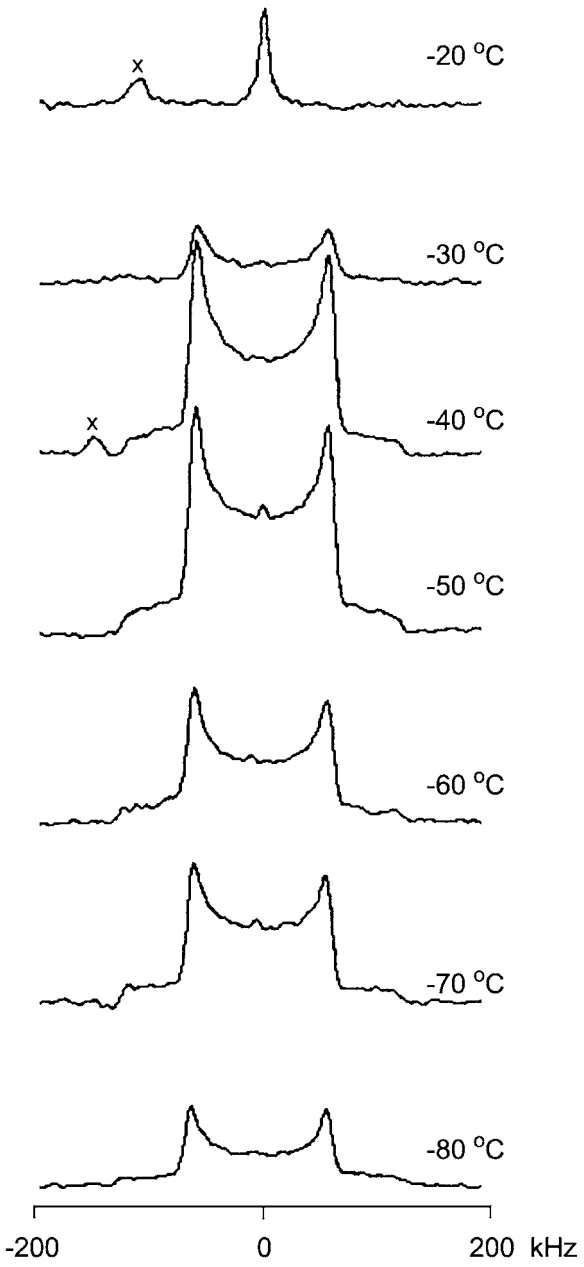

Figure 2. One-dimensional spectra of D-ribose-2′-*d* recorded at temperatures between −20 °C and −80 °C. A total of 1024 scans were recorded per spectrum. The '×' indicates the positions of spectral artifacts.

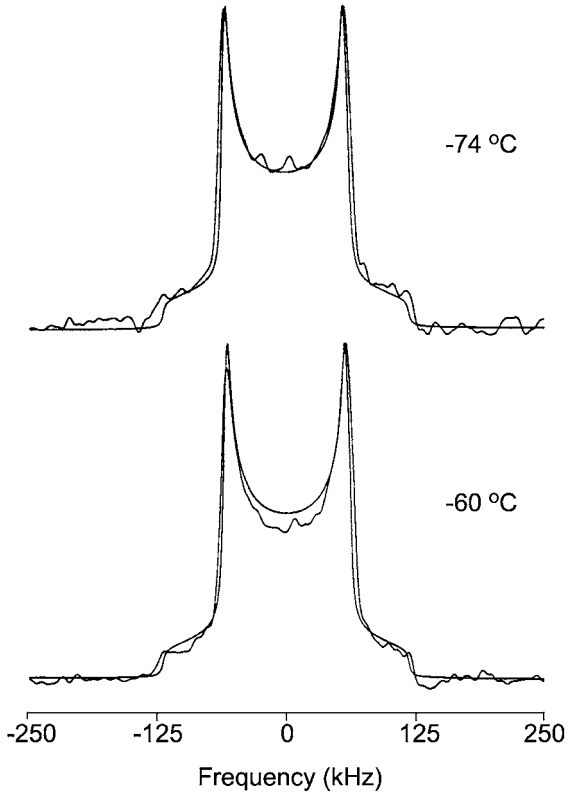

Figure 3. ^{2}H quadrupole line shapes of D-ribose-2′-*d* at −60 and −74 °C with the same static line shape simulation superimposed. The line shape was simulated using values of $QCC_{\text{eff}} = 162$ kHz and $\eta_{\text{eff}} = 0.04$. A total of 1024 transients per spectrum were recorded.

shown), indicating that the ribose molecules were highly constrained within the crystalline lattice, and prevented initial attempts to collect quadrupolar echo and deuterium relaxation measurements under these conditions. X-ray powder diffraction data of anhydrous D-ribose, shown in Figure 1A, confirmed it to be in the crystalline state. Thus, in order to alleviate long NMR relaxation times and to eliminate crystal-packing forces, all NMR data on D-ribose-2′-*d* presented here were recorded under partially hydrated conditions (average of 3.1 waters per ribose molecule). X-ray powder diffraction data on D-ribose hydrated with an average of only 1.4 waters per ribose molecule, shown in Figure 1B, revealed that the sample was composed of both amorphous and crystalline components. NMR spectra of D-ribose-2′-*d* at or above −20 °C revealed an isotropically-averaged line shape (Figure 2), which was from rapidly reorienting ribose molecules present in the amorphous,

deliquesced part of the sample. The absence of a Pake doublet pattern at or above −20 °C indicated that the crystalline component of the sample did not contribute to our NMR spectra.

Shown in Figure 3 are experimental 61.4 MHz ^{2}H NMR quadrupole echo line shapes of D-ribose-*2′-d* at −74 and −60 °C. Both spectra had a classic Pake doublet pattern with a quadrupole splitting of 122 ± 2 kHz. Both spectra were well fit using a line shape simulation with $QCC_{\text{eff}} = 162$ kHz and $\eta_{\text{eff}} = 0.04$. The size of the quadrupole splitting indicated the absence of fast, large amplitude motions in D-ribose-*2′-d* at −60 and −74 °C and were the same as those of crystalline deoxythymidine-*2′-C*,*2″-C-d*$_2$ (Hiyama et al., 1989) and [2″-^{2}H]-2′-deoxycytidine of C3 of d[(CGCGAATTCGCG)]$_2$ at low hydration (Meints et al., 2001).

Powder averaged spin-lattice relaxation times of ^{2}H of D-ribose-*2′-d* were measured at seven different temperatures between −50 and −90 °C and ranged from 1.1 ± 0.1 s at −50 °C to 6.2 ± 0.1 s at −90 °C. Typical saturation-recovery plots are shown in Figure 4, which were collected at −60 and −70 °C and yielded $\langle T_1 \rangle$ values of 1.2 ± 0.1 and 3.6 ± 0.1 s, respectively. In Figure 5 the spin-lattice relaxation times are shown in an Arrhenius plot, yielding an apparent activation energy of 3.6 ± 0.7 kcal mol^{-1}. Also shown are spin-lattice relaxation times of crystalline deoxythymidine-*2′-C*,*2″-C-d*$_2$ taken from Hiyama et al. (1989) that were used to obtain an apparent activation energy of 3.8 kcal mol^{-1}. Comparable spin-lattice relaxation times and line shapes to those of Hiyama et al. indicated that D-ribose-*2′-d* experienced fast internal motions similar to those of crystalline deoxythymidine, but under non-crystalline conditions. Hiyama et al. (1989) postulated that the activation energy corresponded to conformational exchange between C2′-*endo* and C3′-*exo* conformations that modulated the C2′–H2′ vector by a small amplitude ($\leq 5°$ r.m.s.).

The ^{2}H spin-lattice relaxation times of the hydrated, non-crystalline D-ribose-*2′-d* were such that an investigation of slow motions using spin-alignment experiments (Lausch and Spiess, 1980; Spiess, 1980) was feasible. The spin alignment experiment is particularly well suited for detecting slow jump processes of the kind that might be expected for sugar puckering motions in nucleic acids. For a slow motion corresponding to an N-site jump among equally populated sites, the spin-alignment echo intensity is predicted to rapidly decay exponentially to $1/N$ of its initial intensity with a time constant τ_c and then slowly decay exponentially with a time constant of $\langle T_{1Q} \rangle$, as described by $S(\tau_2) = (1-f)\exp(-\tau_2/\tau_c - \tau_2/\langle T_{1Q}\rangle) + f\exp(-\tau_2/\langle T_{1Q}\rangle)$, where $f = 1/N$ and τ_2 is the period of the pulse sequence during which spin alignment is allowed to relax (Hiyama et al., 1989). In contrast, slow diffusive motions, where $N \rightarrow \infty$, result in a rapid exponential decay of the spin alignment echo to zero intensity with time constant τ_c. Shown in Figure 6 are spin alignment echo heights of D-ribose-*2′-d* at −74 and −60 °C as a function of the τ_2 period. Despite the similarity in the line shapes at these two temperatures (Figure 3), the data in Figure 6 revealed the presence of two different types of slow motions of the C2′–H2′ bond of D-ribose. The spin alignment echo at −74 °C displayed a biexponential decay with a rapid decay of the echo amplitude to 50% of its initial intensity, indicating that $N = 2$. At −60 °C, however, the echo intensity vanished in less than 10 ms, indicating that N assumed a large value consistent with a diffusion motion. The rapid decay rate could not be due to spin-lattice relaxation because $\langle T_1 \rangle = 1.2 \pm 0.1$ s at this temperature. The data in Figure 6 indicated that between −60 and −74 °C, the slow internal motion of the C2′-H2′ bond of D-ribose made a transition from a diffusive process to that of a two-site jump, respectively. Therefore, in a hydrated, non-crystalline form, the ribose ring, totally free of substituents, appeared to execute a two-site jump, provided enough thermal energy was removed from the system. In an effort to estimate the internal correlation time of the jump motion of C2′–H2′ at −74 °C, the data was fit to the equation for $S(\tau_2)$ given above. Based on a two-site jump model between two equally populated sites the values of τ_c and $\langle T_{1Q} \rangle$ were determined to be 0.24 ± 0.04 ms and 1.2 ± 0.3 s, respectively. The fit is shown as a solid line in Figure 6.

In principle, a two-dimensional spin-alignment experiment (Schmidt et al., 1986) can provide a direct measurement of the angle between the two vectors undergoing exchange. However, we were unable to collect sufficient signal-to-noise in order to observe magnetization exchange directly in the two-dimensional spin-alignment spectrum. Alternatively, we investigated the quadrupole echo line shapes for a few different values of the τ_1 evolution time using $\tau_2 = 1.4$ ms at −74 °C. The horns and shoulders of the Pake powder pattern showed little sign of decay in their intensity (Figure 7, top), consistent with the slow millisecond jump process indicated from the data in Figure 6. The spectra collected at −60 °C at half

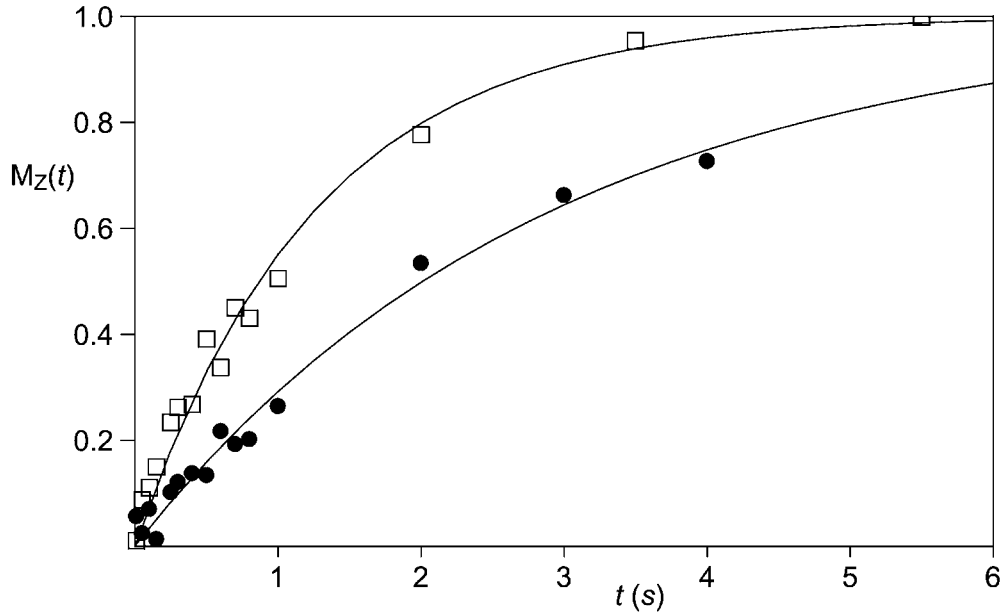

Figure 4. Saturation-recovery data of D-ribose-2′-*d* at −60 and −70 °C. The −60 °C (open squares) and −70 °C (solid circles) data were fit with single exponentials, as shown here, and resulted in ^{2}H $\langle T_1 \rangle$ times of 1.2 ± 0.1 and 3.6 ± 0.1 s, respectively. Echo intensities were normalized to those obtained without a saturating comb of 90° pulses.

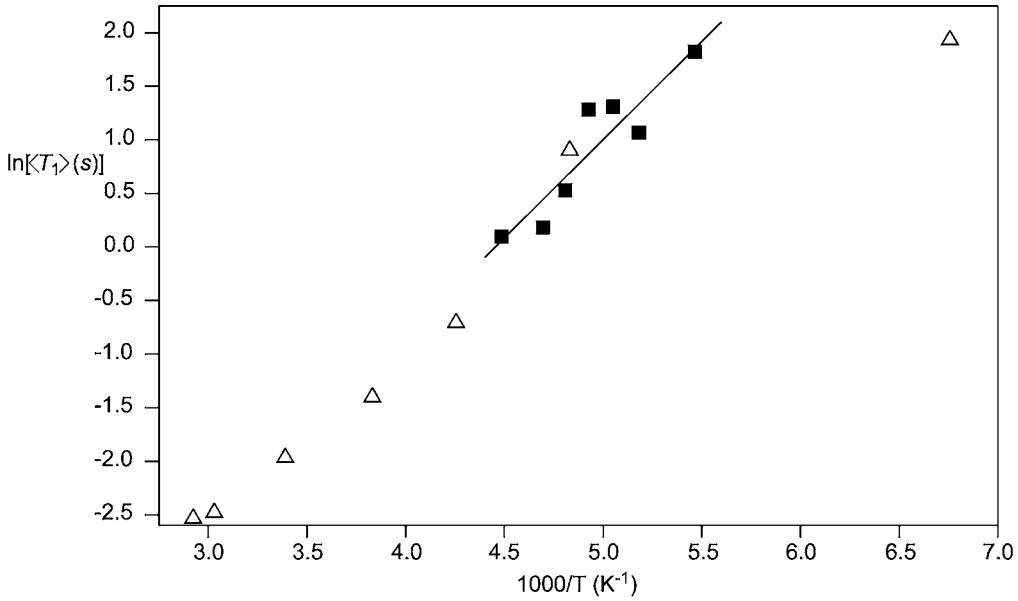

Figure 5. Arrhenius plot of ^{2}H $\langle T_1 \rangle$ values of D-ribose-2′-*d*. Data collected here on D-ribose-2′-d are shown as solid squares. Open triangles represent data taken from Hiyama et al. (1989). The line represents a fit to the $\langle T_1 \rangle$ values of D-ribose-2′-d and yielded an activation energy of 3.6 ± 0.7 kcal mol^{-1}.

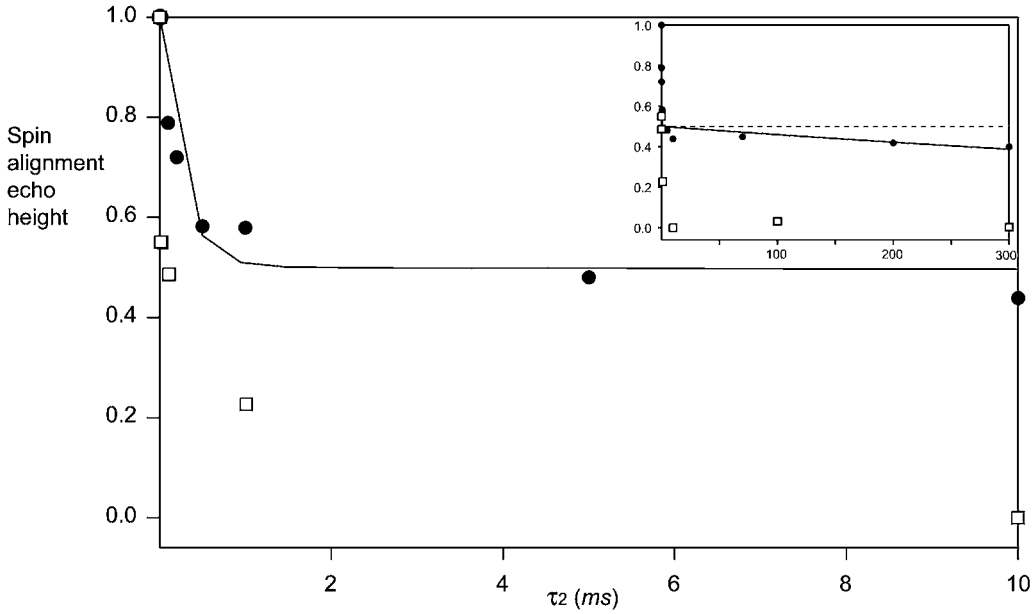

Figure 6. Spin alignment echo intensities of D-ribose-2′-*d* plotted as a function of the τ_2 period (0–10 ms) at −74 (solid circles) and −60 °C (open squares). Spectra were collected using $\tau_1 = 25$ μs. The inset shows the entire τ_2 range (0–300 ms). The dotted line indicates where the signal intensity is half of that at $\tau_2 = 0$. The solid line was obtained from a fit to the data collected at −74 °C using the equation $S(\tau_2) = (1 - f)\exp(-\tau_2/\tau_c - \tau_2/\langle T_{1Q}\rangle) + f\exp(-\tau_2/\langle T_{1Q}\rangle)$. Setting $f = 0.5$ yielded values of 0.24 ± 0.04 ms and 1.2 ± 0.3 s for τ_c and $\langle T_{1Q}\rangle$, respectively.

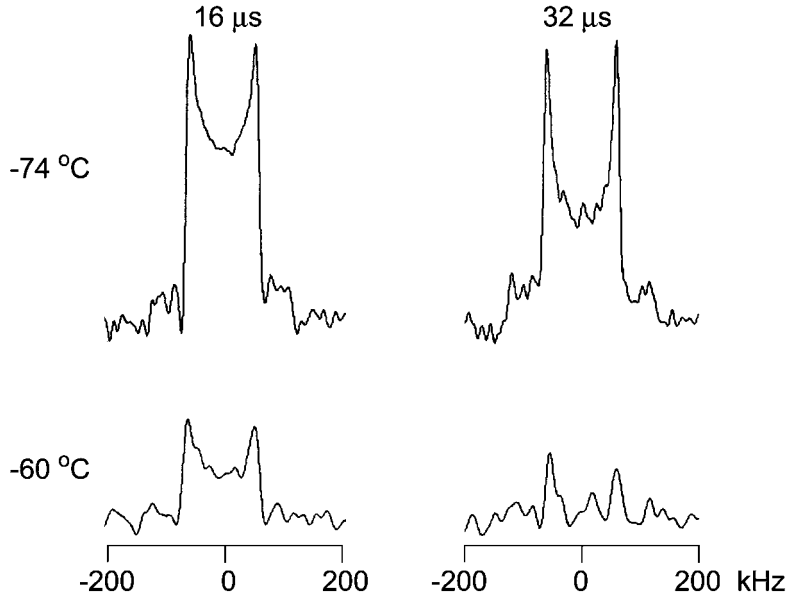

Figure 7. ^{2}H spin alignment spectra of D-ribose-2′-*d* collected at −60 and −74 °C using τ_1 periods of 16 and 32 μs. Mixing times were 0.75 and 1.4 ms and 1024 and 864 transients were recorded at −60 and −74 °C, respectively.

the mixing time ($\tau_2 = 0.75$ ms) exhibited a dramatic loss in intensity over the τ_2 period, consistent with a diffusive process on a short timescale relative to the mixing time, and also showed signs of T_2 distortion with variable τ_1 values, consistent with the presence of a diffusive motion of the C2′–H2′ vector of D-ribose-*2′-d* on the microsecond timescale (Figure 7, bottom). Such T_2 distortions have also been observed in crystalline deoxythymidine-*2′-C*,*2″-C-d*$_2$ and were interpreted as being due to microsecond motions with $\geq 30°$ r.m.s. amplitude (Hiyama et al., 1989). Below −74 °C, spin alignment data was not collected over a sufficiently broad temperature range for calculation of the activation energy for the slow, large amplitude motion. However, it must be higher than 3.6 ± 0.7 kcal mol^{-1} (Figure 5) because the correlation time was substantially longer than that of the small-amplitude nanosecond motion (Figure 6). Thus, a lower limit of the activation energy of the slow motion can be estimated to be ∼4 kcal mol^{-1}. Hiyama et al. (1989) used spin alignment experiments to show that below +55 °C, a slow, large-amplitude motion consistent with that of a two-site jump was present in crystalline deoxythymidine at the 2′ position. However, since the large-amplitude motion was different when the sample included Tris, it was concluded that crystal-packing forces were an important determinant. In part, due to this observation, we prepared the sample of D-ribose-*2′-d* in a partially hydrated state.

It was important to ensure that the transition from a diffusive to a jump process was not related to a phase transition in frozen ice in going from −60 to −74 °C. Wittebort et al. (1988) have shown that water molecules in normal hexagonal ice execute jumps on a tetrahedron at both −60 and −70 °C at 8000 and 2000 s^{-1}, respectively. Therefore, we presumed that the interaction of water with ribose, and its effect on conformational interconversions, was similar at both temperatures.

Conclusions

The data presented here provide evidence that ring puckering in unsubstituted ribose undergoes a transition from a diffusive to a jump process as thermal energy is removed from the system in going from −60 to −74 °C. The lower limit for the activation energy for ring puckering was estimated to be ∼4 kcal mol^{-1}. At −60 °C the motion of the C2′–H2′ bond was diffusive on the microsecond timescale, but at −74 °C the bond jumped between two equally populated sites on the millisecond time scale. Our results are consistent with pseudorotational energies calculated earlier for ribose, which showed that the C2′-*endo* and C3′-*endo* states are equally favorable and separated by a potential energy barrier of ∼3.9 kcal mol^{-1} (Olson, 1982). The local maximum corresponded to the O4′-*endo* conformation and was calculated to be the result of repulsive van der Waals forces between eclipsed 2′- and 3′-hydroxyl groups. In addition to the slow, large-amplitude motions, C2′–H2′ of D-ribose-*2′-d* also executed nanosecond timescale motions of small amplitude with an activation energy of 3.6 ± 0.7 kcal mol^{-1}, which were probably librations of the C2′–H2′ bond within the C2′-*endo* and C3′-*endo* potential energy minima. Fast small-amplitude and slow large-amplitude motions were also found at the C2′–H2′/H2″ bonds in deoxythymidine with similar apparent activation energies (Hiyama et al., 1989), which indicate that the substituents of sugar rings of nucleosides do not greatly impact the fundamental dynamic and energetic properties inherent within an unsubstituted furanose ring. However, solid-state ^{2}H NMR studies of DNA have shown that furanose dynamics is strongly modulated by sequence context and have been observed to execute diffusive as well as jumping motions (Hatcher et al., 1998; Meints et al., 2001).

Acknowledgements

We are thankful for helpful comments by Ioannis Vakonakis. Financial support was provided to A.C.L. by Robert A. Welch Foundation Grant A-1471. G.P.D. acknowledges support by NIH grant R01 GM58914-01. Work by M.A.K. was performed under the auspices of the U.S. Department of Energy (Contract DE-AC06-76RLO1830) and was supported by the Department of Energy Office of Biological and Environmental Research Program under Grant 249311 KP11-01-01. Acquisition and processing of powder diffraction data were performed at the Environmental Molecular Sciences Laboratory (a national scientific user facility sponsored by the U.S. DOE Office of Biological and Environmental Research) located at Pacific Northwest National Laboratory and operated by Battelle for the Department of Energy (contract KP130103). MAK was supported by the Department of Energy Office of Health and Environmental Research Program under grant 22567 KP14-02-01 (PNNL).

References

Arnott, S. and Hukins, D.W.L. (1972) *Biochem. Biophys. Res. Commun.*, **47**, 1504–1510.

Bax, A. and Lerner, L. (1988) *J. Magn. Reson.*, **79**, 429–438.

Davis, J.H., Jeffrey, K.R., Bloom, M., Valic, M.I. and Higgs, T.P. (1976) *Chem. Phys. Lett.*, **42**, 390–394.

Dickerson, R.E. (1983) *J. Mol. Biol.*, **166**, 419–441.

Hatcher, M.E., Mattiello, D.L., Meints, G.A., Orban, J. and Drobny, G.P. (1998) *J. Am. Chem. Soc.*, **120**, 9850–9862.

Hiyama, Y., Roy, S., Cohen, J.S. and Torchia, D.A. (1989) *J. Am. Chem. Soc.*, **111**, 8609–8613.

Kojima, C., Ono, A., Kainosho, M. and James, T.L. (1998) *J. Magn. Reson.*, **135**, 310–333.

Lausch, M. and Spiess, H.W. (1980) *Chem. Phys. Lett.*, **71**, 182–186.

Levitt, M. and Warshel, A. (1978) *J. Am. Chem. Soc.*, **100**, 2607–2613.

Meints, G.A., Karlsson, T. and Drobny, G.P. (2001) *J. Am. Chem. Soc.*, **123**, 10030–10038.

Olson, W.K. (1982) *J. Am. Chem. Soc.*, **104**, 278–286.

Olson, W.K. and Sussman, J.L. (1982) *J. Am. Chem. Soc.*, **104**, 270–278.

Robinson, B.H., Mailer, C. and Drobny, G.P. (1997) *Annu. Rev. Biophys. Biomol. Struct.*, **26**, 629–658.

Roder, O., Ludemann, H. and Goldhammer, E.V. (1975) *Eur. J. Biochem.*, **53**, 517–524.

Saenger, W. (1984) *Principles of Nucleic Acid Structure*, Springer-Verlag, New York, NY.

Saenger, W., Hunter, W.N. and Kennard, O. (1986) *Nature*, **324**, 385–388.

Schmidt, C., Wefing, S., Blumich, B. and Speiss, H.W. (1986) *Chem. Phys. Lett.*, **130**, 84–90.

Spiess, H.W. (1980) *J. Chem. Phys.*, **72**, 6755–6762.

Wang, A.C., Kennedy, M.A., Reid, B.R. and Drobny, G.P. (1992) *J. Am. Chem. Soc.*, **114**, 6583–6585.

Weast, R.C. (Ed.) (1988) *CRC Handbook of Chemistry and Physics*, 1st Student edn. CRC Press, Inc., Boca Raton.

Wittebort, R.J., Usha, M.G., Ruben, D.J., Wemmer, D.E. and Pines, A. (1988) *J. Am. Chem. Soc.*, **110**, 5668–5671.